

Cite as: *Angew. Chem. Int. Ed.* 2019, 58, 2310–2315

A Three-Dimensional Dynamic Supramolecular “Sticky Fingers” Organic Framework

Estefania Fernandez-Bartolome, Jos8 Santos, Arturo Gamonal, Saeed Khodabakhshi, Laura J. McCormick, Simon J. Teat, E. Carolina Saçudo, Jos8 S#nchez Costa,* and Nazario Mart#n*

Abstract: Engineering high-recognition host–guest materials is a burgeoning area in basic and applied research. The challenge of exploring novel porous materials with advanced functionalities prompted us to develop dynamic crystalline structures promoted by soft interactions. The first example of a pure molecular dynamic crystalline framework is demonstrated, which is held together by means of weak “sticky fingers” van der Waals interactions. The presented organic-fullerene-based material exhibits a non-porous dynamic crystalline structure capable of undergoing single-crystal-to-single-crystal reactions. Exposure to hydrazine vapors induces structural and chemical changes that manifest as toposelective hydrogenation of alternating rings on the surface of the [60]fullerene. Control experiments confirm that the same reaction does not occur when performed in solution. Easy-to-detect changes in the macroscopic properties of the sample suggest utility as molecular sensors or energy-storage materials.

One of the important challenges in chemical science nowadays is the search for greener processes for a cleaner world.^[1] In chemistry, this usually translates into highly selective reactions with high rates and efficiencies.^[2] Recently, novel synthetic strategies were proposed that diverge from classical approaches. While the latter are usually based on the temperature, pressure, and exact formulation control, reac-

tivity control of the former explores novel environmental strategies (for example, the successful surface chemistry approach,^[3] chemical topology,^[4] or chemical reactions performed in confined spaces^[5] in which the reactivity differs in many aspects from those conducted in bulk solution). In that sense, porous materials connected by intermolecular bonds (such as, metal–organic frameworks^[6] (MOFs), covalent organic frameworks^[7] (COFs), or porous molecular materials^[8] that are built from discrete molecules^[9] such as porous organic cages)^[10] have provided notable results. The discovery and development of these materials has spurred an interest in confined chemical reactions to determine how spatial confinement can influence the yields and reactivity pathways of reactions.^[11] MOFs offer improved flexibility compared to rigid zeolites and less processable COFs.^[12] This flexibility could generate novel dynamic adsorption properties under realistic conditions—similar to the liquid–protein reactions that occur for specific interactions between an enzymatic host and a substrate. Pure organic systems usually demonstrate excellent properties, such as high thermal stabilities, tunable structural properties, and biocompatibility; however, they also present drawbacks, such as rigidity and limited processability. Therefore, the formation of dynamic structures (porous or non-porous acting as porous) by means of supramolecular interactions between molecules might be an interesting alternative. However, the crystallization of stable organic structures possessing porosity or showing the ability to incorporate molecules by internal structural reorganization (breathing effect) is still a real challenge, with some examples reported using hydrogen bonding^[8,13–22] or p–p stacking^[8,23–25] as a driving force.

In this manuscript, we report for the first time how a flexible non-porous organic molecule connected through supramolecular van der Waals interactions, so-called “sticky fingers”,^[26] behaves as an excellent dynamic molecular receptor. Furthermore, the inclusion of small molecules inside this material allows an unprecedented hydrogenation reaction that occurs only in a confined crystalline space and not by traditional wet chemistry. The reaction is performed in a single-crystal-to-single-crystal (SCSC) fashion, which has allowed us to study how this material behaves upon the inclusion of these small molecules with atomic detail.^[27]

To study this process we have used one of the most versatile organic molecules, namely the [60]fullerene. These highly functionalized [60]fullerene cycloadducts are very appealing scaffolds for the construction of 3D crystalline materials because of the directionality of their malonate substituents.^[20,28–31] The hexakis adduct has been synthesized

[*] E. Fernandez-Bartolome, Dr. J. Santos, Dr. A. Gamonal, Dr. S. Khodabakhshi, Dr. J. S. Costa, Prof. Dr. N. Mart#n
IMDEA Nanociencia, C/ Faraday 9
Ciudad Universitaria de Cantoblanco
28049 Madrid (Spain)
E-mail: jose.sanchezcosta@imdea.org
nazmar@quim.ucm.es

Dr. L. J. McCormick, Dr. S. J. Teat
Advanced Light Source, Berkeley Laboratory
1; Cyclotron Road, Berkeley, CA 94720 (USA)

Dr. E. C. Saçudo
Departament de Qu#mica Inorg#nica i Org#nica, Seccik qu#mica
Inorg#nica, Univ. de Barcelona
Av. Diagonal 645, 08028 Barcelona (Spain),
and
Institut de Nanoci#ncia i Nanotecnologia, Universitat de Barcelona
08028 Barcelona (Spain)

Prof. Dr. N. Mart#n
Departamento de Qu#mica Org#nica
Facultad de Ciencias Qu#micas, Universidad Complutense
28040 Madrid (Spain)

Supporting information and the ORCID identification number(s) for the author(s) of this article can be found under:
<https://doi.org/10.1002/anie.201812419>.

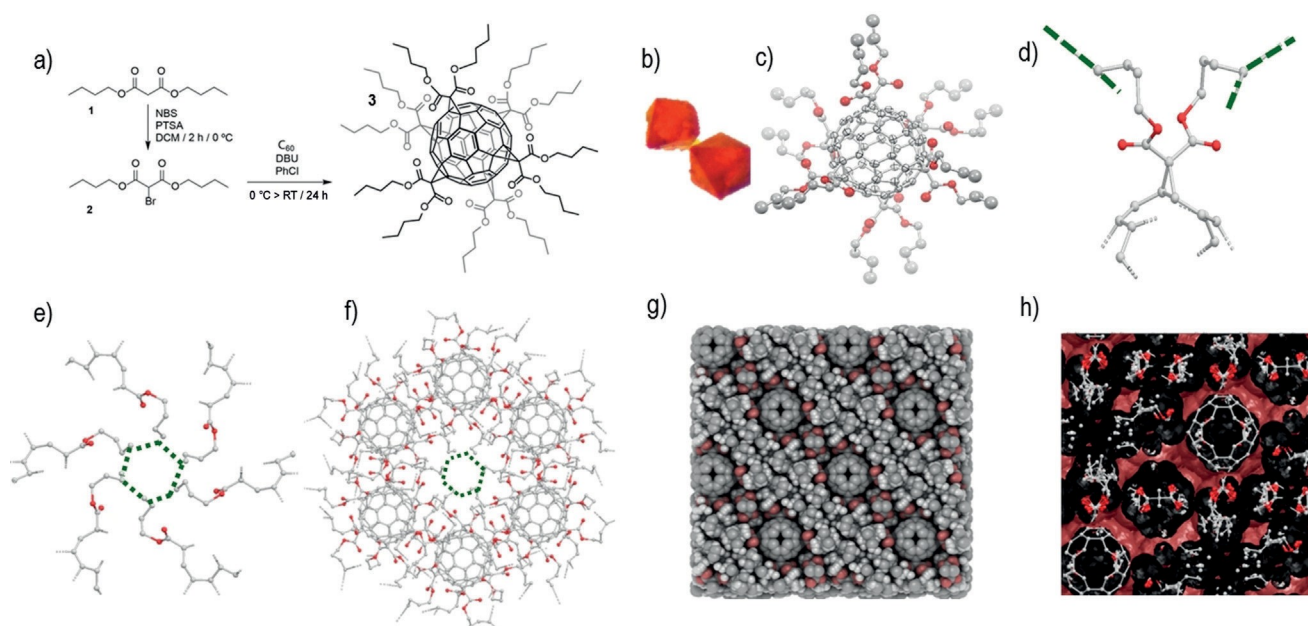


Figure 1. a) Synthesis of **3**; *N*-bromosuccinimide (NBS), *p*-toluenesulfonic acid (PTSA), dichloromethane (DCM), 1,8-diazabicyclo[5.4.0]undec-7-ene (DBU). b) Orange-red single crystals of **3**. c) An ORTEP^[32] illustration of a single hexakis adduct of [60]fullerene, including the malonate groups (only one branch of the distorted malonate structure is illustrated for clarity). d) A depiction of the van der Waals connections of a single malonate group with its close neighbors (the bond direction is plotted as a deep-green dashed line). e) An expansion of the connection network illustrated in (d) with [60]fullerene units omitted for clarity. f) The same six interacting malonate groups illustrated in (e) accompanied by their corresponding C₆₀ buckyballs. g) An iRASP^[33] view of the packing and the h) surface occupancy calculated with OLEX2^[34] highlighting the potential cavities surrounding the [60]fullerene in red.

by applying the well-known Bingel–Hirsch synthetic strategy^[35,36] (see reaction scheme in Figure 1 a). The synthesis was carried out by the addition of the previously obtained bromomalonate (**2**) to a solution of C₆₀ in chlorobenzene by employing DBU as a chemical base. This straightforward and reproducible method affords compound **3** in good yield (45 %). Upon purification, the resulting hexaadduct was characterized by the usual analytical and spectroscopic techniques (see the Supporting Information for further details). Crystallization of **3** from ethanol was achieved using the pressure tube technique (as described in the Supporting Information). This method afforded large, regular, orange crystals that were suitable for X-ray diffraction analysis (Figure 1b; for full synthetic details see the Supporting Information).

Compound **3** crystallized in the cubic space group $Fd\bar{3}$ (Figure 1 c). The unit cell is composed of eight symmetry-equivalent hexaadducts placed in four unequal layers. Importantly, in contrast to the major packing driving force of pristine [60]fullerene,^[37] in **3** there is no evidence of any supramolecular p–p contacts between neighboring fullerene buckyballs (Figure 1g; Supporting Information, Table S2). For **3**, the shortest separation between two adjacent fullerenes placed in different layers is 5.2 c, which is utterly out of the range of supramolecular p–p interactions.^[38,39] Furthermore, the separation between fullerene entities located on the exact same position along the same axis is very long (26.879 c) and is separated by five layers of fullerenes at different heights in the perpendicular axis; thereby, precluding any possible p–p interactions. Altogether, it is considered that the packing

force must be driven by another kind of non-covalent interaction.

From the single-crystal XRD structure of **3** we can observe that six butyl malonate groups are clearly distorted. Each -COOR group is placed over three positions, giving rise to four different butyl branches (two of the branches coming from the same C₆₀-COOR group), for a total of 48 different positions over the whole packing. Figures 1 e–g reveal the intricacy of the hexakis–fullerene network and the interdigitated arrangement of the interacting butyl chains. Figures 1 d–f depict one of these interactions, as well as a network view of the crystal packing created by the hexaadducts through this interaction. The different occupancy factors and the contacts between carbon atoms for this interaction, and for the entire intricate network, are detailed in the Supporting Information. Thus, the main information stemming from this crystallographic study is that these branches create a densely packed 3D structure maintained by van der Waals contacts established between the alkyl chains of neighboring hexakis-[60]fullerenes.

Interestingly, a close look at the crystallographic data confirms that the densely packed 3D structure of fullerene-based **3** shows small cavities that mainly surround the buckyball (Figure 1 h, in red). Despite the presence of small cavities within the structure of the material, the closely packed aliphatic butyl chains prevent volatile molecules from diffusing through the crystal network, as indicated by a Brunauer–Emmett–Teller (BET) surface area value close to zero (see preceding text for details).

To test the absorption of small molecules and the potential subsequent physical changes, single crystals of **3** were exposed to a number of organic and inorganic volatiles. Interestingly, exposure to hydrazine vapors led to an outstanding color change after 3 days at 67 °C. The bright red crystals fade to a pale yellow color (Figure 2 a). The resulting **4**—obtained by a SCSC reaction—presents a structure closely related to **3**, which agrees with a $C_{126}H_{132}O_{24}$ formulation containing 24 more hydrogen atoms than in **3** ($C_{126}H_{108}O_{24}$).

The new material is stable under atmospheric conditions and highly soluble in common organic solvents such as dichloromethane, chloroform, and acetone. To our delight, the structure of **4** was verified by both single-crystal and crystalline powder XRD studies. Complex **4** retains the same space group as its precursor, although the value of the axis diminishes from 26.878(1) to 26.156(3) Å (Supporting Information, Table S1). From the X-ray crystal structure of **4**, it is concluded that half of the six-membered rings associated with [60]fullerene in **3** have been hydrogenated after the exposure of the crystals to the hydrazine vapors (Figures 2 a,d,e, hydrogen atoms are denoted in black). Remarkably, under these reaction conditions only half of the accessible six-membered rings are hydrogenated. Interestingly, the partial hydrogenation of **3** always takes place with preservation of the symmetry of the molecule, which is also evident in the extremely simple ^{13}C NMR pattern observed (Figure 3). This result has been reproduced several times and the same hydrogenation pattern is always obtained. As a result of partial hydrogenation the fullerene cage experiences a strong distortion, which arises from the sp^2 to sp^3 hybridization change of the hydrogenated six-membered rings. The XRD data show an increase of the C@C bonding distances, along with a decrease of the hybridization angle of the involved

carbon atoms (Figures 2 b–d; Supporting Information, Figure S18). Like its parent molecule (**3**), the hydrogenated hexakis adduct (**4**) crystals are non-porous (Figure 2 f).

Characterization of **3** and **4** was carried out by standard spectroscopic techniques and was greatly facilitated by the high symmetry of the complexes. The 1H NMR spectra of **3** and **4** are shown in Figure 3 and are described in detail in the Supporting Information. Thus, the 1H NMR spectrum of **3** displays four signals at 4.33, 1.68, 1.41, and 0.92 ppm that are consistent with 12 butyl malonate groups. The hydrogenation of **3** is clearly evident in the 1H NMR spectrum where two nearly isochronous signals emerge at 3.58 ppm that integrate to 24 protons. This is consistent with the total hydrogenation of four of the eight six-membered rings of **3**. Jointly with a $^{135}DEPT$ (distortionless enhancement by polarization transfer) experiment, the C@H correlations found by heteronuclear single quantum coherence spectroscopy (HSQC) allow these new H signals to be correlated with methyne carbon atoms on the fullerene surface. The environment changes induced upon hydrogenation cause an upfield shift in the $-COOCH_2-$ methylene resonances from 4.33 to 4.20 ppm. Furthermore, this signal also shows signs of splitting—probably as a consequence of methylene groups lying over hydrogenated and unsaturated rings.

As for precursor **3**, the ^{13}C NMR spectrum of **4** shows a fine and simple pattern derived from the high symmetry of the complex. As a consequence of this symmetry, all the sp^2 carbons belonging to the fullerene cage manifest as two signals at 144.0 and 134.3 ppm (significantly shielded compared to the parent complex **3**, at 145.8 and 141.3 ppm, respectively). The signals of the hydrogenated sp^3 carbons appear as two peaks at 39.8 and 35.5 ppm (correlating with the protons at 3.58 ppm). Mass spectrometry analysis confirms

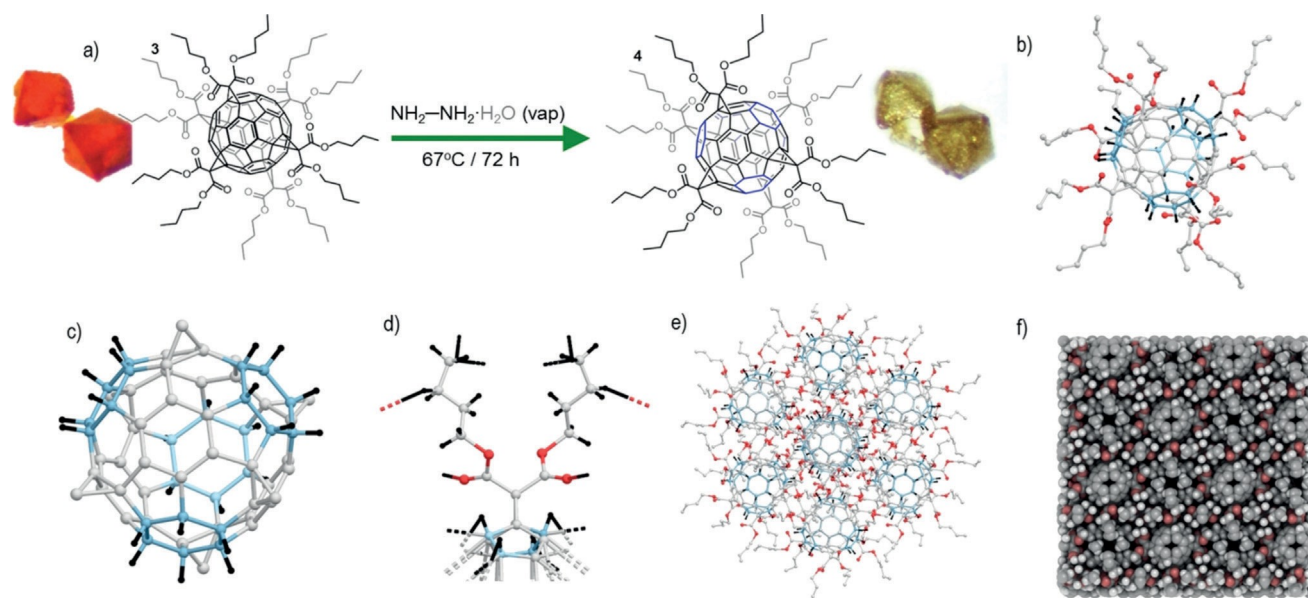


Figure 2. a) Synthesis of **4** by the SCSC reaction, including a picture of the crystal after (top) and before (bottom) exposure to hydrazine vapors. b) A crystal structure visualization of the hydrogenated hexakis adduct in Mercury,^[40] including the hydrogen atoms contained within C_{60} and the malonate functional groups (only one branch of the distorted malonate is illustrated for clarity). c) A view of the C_{60} hydrogenated fullerene with the added hydrogen atoms distinguished in black. d) A depiction of the van der Waals interactions between a single malonate group and its close neighbors. e) Expansion of the connection network including the C_{60} buckyballs. f) An iRASPA view of **4**.

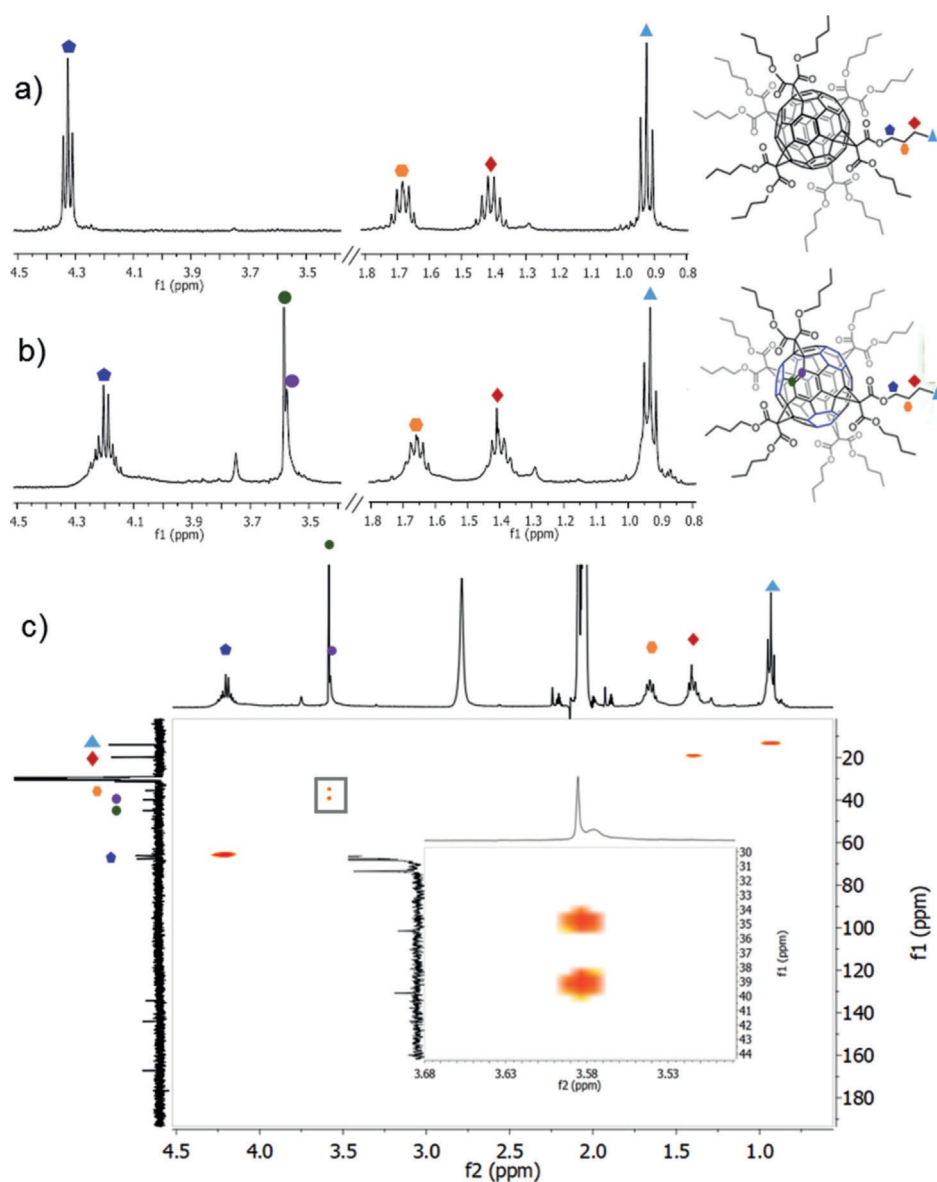


Figure 3. a,b) ^1H NMR spectra of compounds 3 and 4, respectively. c) HSQC NMR spectrum of compound 4 and the amplified HSQC NMR spectrum (inset) of the novel hydrogen signals (3.58 ppm). The resonances of each spectrum have been assigned to key atoms under discussion with symbols and colors.

the presence of the molecular peak of 4 (Supporting Information, Figure S16). Thermogravimetric analysis provides an insight into the thermal stability of hydrogenated compound 4, which is stable up to 150 $^{\circ}\text{C}$ when it starts decomposing. In contrast, non-saturated 3 exhibits high stability and decomposes above 275 $^{\circ}\text{C}$ (Supporting Information, Figure S13). This stability loss is attributed to the increased strain supported by the fullerene cage upon conversion of 24 sp^2 carbon atoms into sp^3 carbon atoms. This is observed in dramatic fashion in the XRD crystal structure, where the cage appears to bulge beyond a spherical shape.

The use of molecular hydrogen in the presence of a metal catalyst is the most recognized method for the hydrogenation of alkenes.^[41] Despite widespread use of catalytic hydro-

genation, exceptional security measures are required for handling molecular hydrogen and expensive catalysts are needed. Hydrazine offers an alternative hydrogen source. Nevertheless, hydrogenation of olefins with hydrazine requires hydrazine decomposition over a metal to yield hydrogen or oxidation to diimide^[42] to yield a reactive species capable of reducing the olefin.

The latter procedure involves a rather unstable diimide intermediate that is extremely short-lived in solution. We believe that the diimide species (generated in situ from the oxidation of hydrazine) is stabilized within the network of 3 as a consequence of confinement inside the pockets surrounding the fullerene moieties. In this environment concerted hydrogen transfer takes place from *cis*-diimide to half of the cyclohexatriene rings remaining on fullerene. Attempts to duplicate this result in solution resulted in either no evolution of the reaction or led to a complex mixture of byproducts—none of them consistent with the chromatographic R_f of 4 (Supporting Information, Figure S4).

The work herein describes the first reported weak van der Waals “sticky fingers” crystalline structure of a [60]fullerene hexakis adduct. These non-covalent (dispersion stabilization) interactions, also known as “sticky fingers”, are established between the non-polar butyl chains linked

to the malonate functionalities. The large number of butyl branches shown in the XRD experiments indicates a dynamic interaction between interdigitating aliphatic chains. The resulting material shows small cavities at the surface of the fullerene, although the overall structure is non-porous. Despite this apparent non-porosity, the dynamic nature of the “sticky fingers” interaction allows for the diffusion of volatiles to the cavities. Interestingly, hydrazine molecules allocated inside these pockets trigger the toposselective hydrogenation of half of the remaining cyclohexatriene rings of the hexaadduct in a SCSC reaction accompanied by a color change into the visible range. We believe that further design of new suitably functionalized hexaadducts will allow materials to be obtained with customizable pockets ready for capturing different volatiles and gases. Therefore, the new

and groundbreaking strategy described in this manuscript on topochemical solid-state reactions involving fullerenes will contribute to the creation of novel carbon-based advanced absorbent materials with a variety of direct technological applications.

Experimental Section

Experimental Details. Preparation of dibutyl 2-bromomalonate (2), [60]fullerene hexakis adduct (3) and hydrogenated fullerene (4) are described in the Supporting Information, along with details pertaining to the XRD and the NMR measurements performed. Crystal Structure Determination: the data for 3 were collected with an orange block crystal with a Bruker APEX II CCD diffractometer at the Advanced Light Source beamline 11.3.1 at Lawrence Berkeley National Laboratory from a Si(111) monochromator ($T=100\text{K}$, $\lambda=0.7749\text{\AA}$). The data for 4 were collected with a yellow block crystal with a MD2M-Maatel diffractometer at the XALOC beamline (BL13) at ALBA Synchrotron with the collaboration of XALOC-ALBA staff, from a Si(111) monochromator. CCDC 1870483 and 1870484 (3, 4) contain the supplementary crystallographic data for this paper. These data can be obtained free of charge from The Cambridge Crystallographic Data Centre.

Acknowledgements

J.S.C. is grateful to the Spanish MINECO for financial support through a National Research Project (CTQ2016-80635-P) and the Ramon y Cajal Research program (RYC-2014-16866) for funding. IMDEA Nanociencia acknowledges support from the "Severo Ochoa" Programme for Centres of Excellence in R&D (MINECO, Grant SEV-2016-0686). E.C.S. acknowledges financial support from the Spanish Government, (Grant CTQ2015-68370-P). This research used resources at the Advanced Light Source, which is a DOE Office of Science User Facility under contract no. DE-AC02-05CH11231. N.M. acknowledges support from the European Research Council (ERC-320441-Chirallcarbon), J.S. and N.M. thank the MINECO of Spain (projects CTQ2017-83531-R and CTQ2016-81911-REDT) and the CAM (FOTOCARBON project S2013/MIT-2841). We are thankful for the use of the XALOC-ALBA synchrotron source under the project no. (2018012561).

Conflict of interest

The authors declare no conflict of interest.

Keywords: fullerenes · single-crystal-to-single-crystal reactions · supramolecular Chemistry · topological chemistry · van der Waals interactions

How to cite: *Angew. Chem. Int. Ed.* 2019, 58, 2310–2315
Angew. Chem. 2019, 131, 2332–2337

- [4] R. S. Forgan, J. P. Sauvage, J. F. Stoddart, *Chem. Rev.* 2011, 111, 5434–5464.
- [5] S. H. Petrosko, R. Johnson, H. White, C. A. Mirkin, *J. Am. Chem. Soc.* 2016, 138, 7443–7445.
- [6] H. Furukawa, K. E. Cordova, M. O'Keeffe, O. M. Yaghi, *Science* 2013, 341, 1230444.
- [7] A. P. Cotter, A. I. Benin, N. W. Ockwig, M. O'Keeffe, A. J. Matzger, O. M. Yaghi, *Science*, 2005, 310, 1166–1171.
- [8] M. I. Hashim, H. T. M. Le, T.-H. Chen, Y.-S. Chen, O. Daugulis, C.-W. Hsu, A. J. Jacobson, W. Kaveevivitchai, X. Liang, T. Makarenko, O. Š. Miljanić, I. Popovs, H. V. Tran, X. Wang, C.-H. Wu, J. I. Wu, *J. Am. Chem. Soc.* 2018, 140, 6014–6026.
- [9] H. Yamagishi, H. Sato, A. Hori, Y. Sato, R. Matsuda, K. Kato, T. Aida, *Science* 2018, 361, 1242–1246.
- [10] T. Hasell, A. I. Cooper, *Nat. Rev. Mater.* 2016, 1, 16053.
- [11] Y. Inokuma, M. Kawano, M. Fujita, *Nat. Chem.* 2011, 3, 349–358.
- [12] A. Schneemann, V. Bon, I. Schwedler, I. Senkovska, S. Kaskel, R. A. Fischer, *Chem. Soc. Rev.* 2014, 43, 6062–6096.
- [13] R. S. Patil, D. Banerjee, C. Zhang, P. K. Thallapally, J. L. Atwood, *Angew. Chem. Int. Ed.* 2016, 55, 4523–4526; *Angew. Chem.* 2016, 128, 4599–4602.
- [14] M. Mastalerz, I. M. Oppel, *Angew. Chem. Int. Ed.* 2012, 51, 5252–5255; *Angew. Chem.* 2012, 124, 5345–5348.
- [15] J. Lg, C. Perez-Krap, M. Suyetin, N. H. Alsmail, Y. Yan, S. Yang, W. Lewis, E. Bichoutskaia, C. C. Tang, A. J. Blake, R. Cao, M. Schröder, *J. Am. Chem. Soc.* 2014, 136, 12828–12831.
- [16] P. K. Thallapally, B. P. McGrail, J. L. Atwood, C. Gaeta, C. Tedesco, P. Neri, *Chem. Mater.* 2007, 19, 3355–3357.
- [17] D. D. Zhou, Y. T. Xu, R. B. Lin, Z. W. Mo, W. X. Zhang, J. P. Zhang, *Chem. Commun.* 2016, 52, 4991–4994.
- [18] R. Natarajan, L. Bridgland, A. Sirikulkajorn, J.-H. Lee, M. F. Haddow, G. Magro, B. Ali, S. Narayanan, P. Strickland, J. P. H. Charmant, A. G. Orpen, N. B. McKeown, C. G. Bezzu, A. P. Davis, *J. Am. Chem. Soc.* 2013, 135, 16912–16925.
- [19] S. M. J. Rogge, A. Bavykina, J. Hajek, H. Garcia, A. I. Olivoso-Suarez, A. Sepfllveda-Escribano, A. Vimont, G. Clet, P. Bazin, F. Kapteijn, M. Daturi, E. V. Ramos-Fernandez, F. X. Llabrés i Xamena, V. VanSpeybroeck, J. Gascon, *Chem. Soc. Rev.* 2017, 46, 3134–3184.
- [20] A. Kraft, J. Stangl, A. Krause, K. Müller-Buschbaum, F. Beuerle, *Beilstein J. Org. Chem.* 2017, 13, 1–9.
- [21] M. Sharafi, J. P. Campbell, S. C. Rajappan, N. Dudkina, D. L. Gray, T. J. Woods, J. Li, S. T. Schneebeli, *Angew. Chem. Int. Ed.* 2017, 56, 7097–7101; *Angew. Chem.* 2017, 129, 7203–7207.
- [22] Y.-L. Wu, N. E. Horwitz, K.-S. Chen, D. A. Gomez-Gualdrón, N. S. Luu, L. Ma, T. C. Wang, M. C. Hersam, J. T. Hupp, O. K. Farha, R. Q. Snurr, M. R. Wasielewski, *Nat. Chem.* 2016, 9, 466–472.
- [23] B. Kohl, F. Rominger, M. Mastalerz, *Org. Lett.* 2014, 16, 704–707.
- [24] S. Dalapati, R. Saha, S. Jana, A. K. Patra, A. Bhaumik, S. Kumar, N. Guchhait, *Angew. Chem. Int. Ed.* 2012, 51, 12534–12537; *Angew. Chem.* 2012, 124, 12702–12705.
- [25] R. G. D. Taylor, C. G. Bezzu, M. Carta, K. J. Msayib, J. Walker, R. Short, B. M. Kariuki, N. B. McKeown, *Chem. Eur. J.* 2016, 22, 2466–2472.
- [26] J. Echeverría, G. Aullón, D. Danovich, S. Shaik, S. Alvarez, *Nat. Chem.* 2011, 3, 323–330.
- [27] J. S. Costa, S. Rodríguez-Jiménez, G. A. Craig, B. Barth, C. M. Beavers, S. J. Teat, G. Aromí, *J. Am. Chem. Soc.* 2014, 136, 3869–3874.
- [28] A. Muçoz, D. Sigwalt, B. M. Illescas, J. Luczkowiak, L. Rodríguez-Pérez, I. Nierengarten, M. Holler, J.-S. Remy, K. Buffet, S. P. Vincent, J. Rojo, R. Delgado, J.-F. Nierengarten, N.

[1] S. Otto, *Chem* 2017, 2, 158–159.

[2] R. Noyori, *Nat. Chem.* 2009, 1, 5–5.

[3] J. I. Urgel, D. Pcija, G. Lyu, R. Zhang, C.-A. Palma, W. Auwarter, N. Lin, J. V. Barth, *Nat. Chem.* 2016, 8, 657–662.

- [29] A. M. Rice, E. A. Dolgoplova, N. B. Shustova, *Chem. Mater.* 2017, 29, 7054 – 7061.
- [30] A. Kraft, F. Beuerle, *Tetrahedron Lett.* 2016, 57, 4651 – 4663.
- [31] A. Kraft, P. Roth, D. Schmidt, J. Stangl, K. Mglger-buschbaum, F. Beurle, *Chem. Eur. J.* 2016, 22, 5982 – 5987.
- [32] L. J. Farrugia, *J. Appl. Cryst.* 2012, 45, 849 – 854.
- [33] D. Dubbeldam, S. Calero, T. J. H. Vlught, *Mol. Simul.* 2018, 7022, 1– 24.
- [34] O. V. Dolomanov, L. J. Bourhis, R. J. Gildea, J. A. K. Howard, H. Puschmann, *J. Appl. Cryst.* 2009, 42, 339 – 341.
- [35] C. Bingel, *Chem. Ber.* 1993, 126, 1957 – 1959.
- [36] I. Lamparth, C. Maichle-Mcßmer, A. Hirsch, *Angew. Chem. Int. Ed. Engl.* 1995, 34, 1607 – 1609; *Angew. Chem.* 1995, 107, 1755 – 1757.
- [37] R. D. Kennedy, M. Halim, S. I. Khan, B. J. Schwartz, S. H. Tolbert, Y. Rubin, *Chem. Eur. J.* 2012, 18, 7418 – 7433.
- [38] A. O'Neil, C. Wilson, J. M. Webster, F. J. Allison, J. A. K. Howard, M. Poliakoff, *Angew. Chem. Int. Ed.* 2002, 41, 3796 – 3799; *Angew. Chem.* 2002, 114, 3950 – 3953.
- [39] M. V. Korobov, A. L. Mirakian, N. V. Avramenko, E. F. Valeev, I. S. Neretin, Y. L. Slovokhotov, A. L. Smith, G. Olofsson, R. S. Ruoff, *J. Phys. Chem. B* 1998, 102, 3712 – 3717.
- [40] C. F. Macrae, I. J. Bruno, J. A. Chisholm, P. R. Edgington, P. McCabe, E. Pidcock, L. Rodriguez-Monge, R. Taylor, J. van de Streek, P. A. Wood, *J. Appl. Cryst.* 2008, 41, 466 – 470.
- [41] B. Mattson, W. Foster, J. Greimann, T. Hoette, N. Le, A. Mirich, S. Wankum, A. Cabri, C. Reichenbacher, E. Schwanke, *J. Chem. Educ.* 2013, 90, 613 – 619.
- [42] B. Pieber, S. T. Martinez, D. Cantillo, C. O. Kappe, *Angew. Chem. Int. Ed.* 2013, 52, 10241 – 10244; *Angew. Chem.* 2013, 125, 10431 – 10434.

Manuscript received: October 30, 2018

Revised manuscript received: November 26, 2018

Accepted manuscript online: December 14, 2018

Version of record online: January 24, 2019